

The impact fracture behaviour of notched specimens of polycarbonate

R. A. W. FRASER, I. M. WARD

Department of Physics, University of Leeds, Leeds, UK

The impact fracture behaviour of notched specimens of polycarbonate has been studied for a range of notch tip radii. For razor-notched specimens a simple fracture toughness analysis is appropriate, as shown by previous workers. Very blunt notches also give constant fracture toughness values, but at a much higher level, corresponding to a different mode of failure. For intermediate notch tip radii the situation is much more complex, and comparison of results for two molecular weight grades shows that the behaviour is molecular weight-dependent. Analysis of these results has been discussed either in terms of a combination of plane strain and plane stress fracture modes, or in terms of a critical stress at the root of the notch, which appears to be appropriate in certain cases.

1. Introduction

In a study of the fracture behaviour of vinylurethane polymers [1], it was noted that the notched and unnotched impact strengths varied in a totally different manner as the chemical composition of the polymers was varied by changing the styrene concentration. In particular, the impact strengths of sharply notched specimens correlated well with the fracture toughness determined in conventional cleavage fracture experiments, whereas the impact strengths of unnotched specimens correlated with the craze stress, as determined from modelling the fracture behaviour in terms of the Dugdale plastic zone. These observations led Brown [2] to undertake a more detailed study of the Charpy impact test for sharply notched specimens, and using experimental data for polymethylmethacrylate (PMMA) he established a direct analysis of the impact test in terms of linear elastic fracture mechanics. Similar work was undertaken independently by Williams *et al.* [3]. Subsequently, Fraser and Ward [4] made an extensive survey of the fracture behaviour of notched specimens of PMMA with varying notch tip radius. Specimens with a wide range of geometries were examined in Charpy impact tests, and also in tensile and slow bend fracture tests. It

was confirmed that the failure of the very sharply notched specimens was consistent with linear elastic fracture mechanics, and defined a constant fracture toughness K_{IC} for a constant notch tip radius. On the other hand, blunt-notched specimens, including standard Charpy notched specimens, failed at a constant critical stress at the root of the notch, a result which brought the impact tests into agreement with Gotham's observations [5] on the tensile fracture of notched samples of PMMA.

The present paper describes an examination of the impact behaviour of notched specimens of polycarbonate (PC). It is less extensive than the previous studies of PMMA in that slow bend and tensile tests were not carried out in view of the ductile failure of PC in such tests at the comparatively slow rates of testing available to us. It is, however, more extensive in that measurements were undertaken on two different molecular weight grades of PC with markedly different fracture behaviour. It will be shown that the behaviour is more complex than that of PMMA, and the comparison of the two grades of polymer provides additional valuable information on the mechanism of the fracture process.

In addition to the links with the previous

investigations already cited, the present studies are also complementary to recent researches on PC by Plati and Williams [6], and by Adams *et al.* [7].

2. Experimental

Impact bend tests were undertaken on a wide range of notched specimens of PC. In addition, uniaxial tensile tests were carried out to determine the yield stress and crazing stress of the PC grades used and that of the PMMA used previously.

2.1. Preparation of specimens

Two grades of Bayer Makrolon were used for these experiments, their grade numbers being 2803 ($\bar{M}_n = 9500$, $\bar{M}_w = 20000$) and 2400 ($\bar{M}_n = 7900$, $\bar{M}_w = 15000$). The former was obtained commercially as large extruded sheet of nominal thickness 0.3 cm, and the latter in specially moulded plaques 50 cm \times 15 cm \times 0.3 cm. As a control on the moulding conditions some 2803 grade was also moulded into plaques but only used in slow tensile cleavage tests, not in these impact tests. It showed exactly the same results in the cleavage tests as the large sheet material regarding craze shape, yielded zone sizes and fracture toughness confirming that the change in properties is a real molecular weight effect, and not a processing effect. We are indebted to Dr D. Sims, E.R.D.E. Waltham Abbey, for providing the specially moulded plaques for us.

The impact specimens were all 5 cm long and 1 cm wide. All specimens were notched on one side at the middle point of their length. To produce very sharp notches a razor blade was pushed slowly into the centre of the side of the specimen. To obtain blunter notches, holes were drilled through the specimen and a jeweller's saw used to cut through from the edge of the specimen to the hole. In all cases the resulting cracks had 0° flank angles. Since the size of the drilled hole may differ from the size of the drill used, particularly for small holes, all specimens were measured for notch length and notch tip radius after manufacture but before testing.

2.2. Impact tests

The impact tests were performed using the Housfield Plastics Impact Tester. This is a Charpy machine, for which there is a set of striking tups of different weights available. These cover a range of fracture energies, and the actual fracture

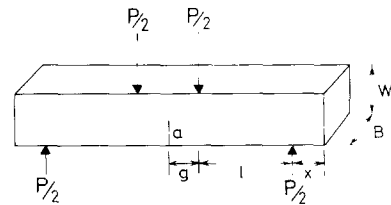


Figure 1 The four-point bend Charpy impact test.

energy in a given test is obtained from calibration charts provided.

The notch tip radii were varied from about 0.018 cm to 0.05 cm and razor notches. In addition the notch depth, a , was varied to give $0 < a/w < 0.6$ where w is the specimen width, so that a set of specimens of different notch length was measured for each value of notch tip radius.

2.3. Uniaxial tensile tests

Uniaxial tensile tests were carried out on dumb-bell specimens, again of 0.3 cm thickness with a gauge length of 3.5 cm and a width in the gauge section of 1 cm. The tests were performed using an Instron tensile testing machine at constant cross-head speeds which gave equivalent strain-rates in the range 4×10^{-6} to $4 \times 10^{-4} \text{ sec}^{-1}$. The craze stress was determined as the stress at which visible crazes were observed throughout the specimen and the yield stress as the nominal stress at the maximum load in the load-extension curve. In fact the craze stress and yield stress are only used for comparative purposes in this paper and actual values are quoted at a strain-rate of $8 \times 10^{-5} \text{ sec}^{-1}$.

3. Theory

Following the approach of the previous paper on PMMA, the failure has been analysed in two ways: either using linear elastic fracture mechanics to calculate the fracture toughness K_{IC} , or by calculating the stress concentration factor to determine the stress at the root of the notch.

3.1. The fracture toughness calculation

If it is assumed that the impact test can be analysed in terms of fracture toughness, the argument first presented by Brown [2] and Marshall *et al.* [3] may be summarized as follows: the elastically stored energy in the specimen immediately prior to failure is given by

$$U_0 = \frac{1}{2} P_0^2 C,$$

where P_0 is the load immediately prior to failure and C is the compliance (relative deflection of the loading points per unit load) of the impact test specimens which is that of a beam deformed as in four-point bending. C is therefore given by the expression

$$C = \frac{18l^2}{E^*BW^2} f\left(\frac{a}{W}\right) + \frac{1}{2E^*BW^3} [4l(3g+1) + 3W^2(1+\nu)]$$

where E^* is the reduced modulus, equal to Young's modulus E , in plane stress conditions, and $E/(1-\nu^2)$ in plane strain (ν is Poisson's ratio), a , W and B are the depth of the notch, the width and breadth of the specimen respectively, l and g are apparatus dimensions and $f(a/W)$ is an integrated function of a/W . The specimen dimensions are shown in Fig. 1.

On this approach of linear elastic fracture mechanics, U_0 , the impact energy, can be simply related to the fracture toughness, K_C , by the Irwin-Kies relationship [8]

$$K_C^2 = \frac{P_0^2}{2B} E^* \frac{dC}{da}$$

To find U_0 , the directly measured value of the impact energy obtained from the Hounsfield calibration charts must be reduced by a small amount which represents the kinetic energy of the specimen itself immediately prior to fracture. In practice, the fracture toughness was obtained by direct calculation from the impact energy and the specimen dimensions using the mathematical analysis.

3.2. Calculation of the maximum stress of the root of the notch

On the assumption that fracture relates to the achievement of a critical stress at the root of the

notch the following argument was proposed [4]. The elastically stored energy immediately prior to fracture is given by

$$U_0 = \frac{1}{2} \left(\frac{2M_0}{l} \right)^2$$

where $M_0 = P_0l/2$ is the applied bending moment immediately prior to fracture.

The maximum stress at the root of the notch at the point of fracture σ_M is then found by multiplying the nominal maximum stress $\sigma_n = 6M_0/[B(W-a)^2]$ by the geometrical stress concentration factor for the particular notch tip radius and length and specimen width involved. The stress concentration factors were taken from the calculations of Neuber [9]. Further details of the exact procedure are given in a previous publication [4].

4. Results and discussion

4.1. Preliminary observations

The impact test results for the higher molecular weight grade of PC are presented in Fig. 2, where each individual result has been analysed as a fracture toughness test along the lines indicated in Section 3.1 above. It can be seen that there is a wide range in the K_C values obtained, and that the results fall into a number of groups. It proved instructive to examine the fracture surfaces in an optical microscope and the key observations are summarized in Fig. 3, together with some useful comparative photographs of PMMA fracture surfaces.

The fracture surfaces of razor-notched and blunt-notched specimens of PMMA are shown in Fig. 3a and b, respectively. All these specimens failed in a brittle manner and the surfaces show the various flat and rough patterns (mirror, mist and hackle) described by previous workers as typical of brittle fracture in a glassy polymer

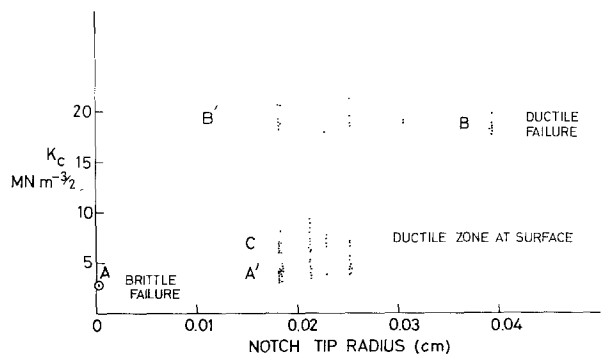


Figure 2 Charpy impact tests on polycarbonate (high molecular weight). Collected data analysed as fracture toughness tests.

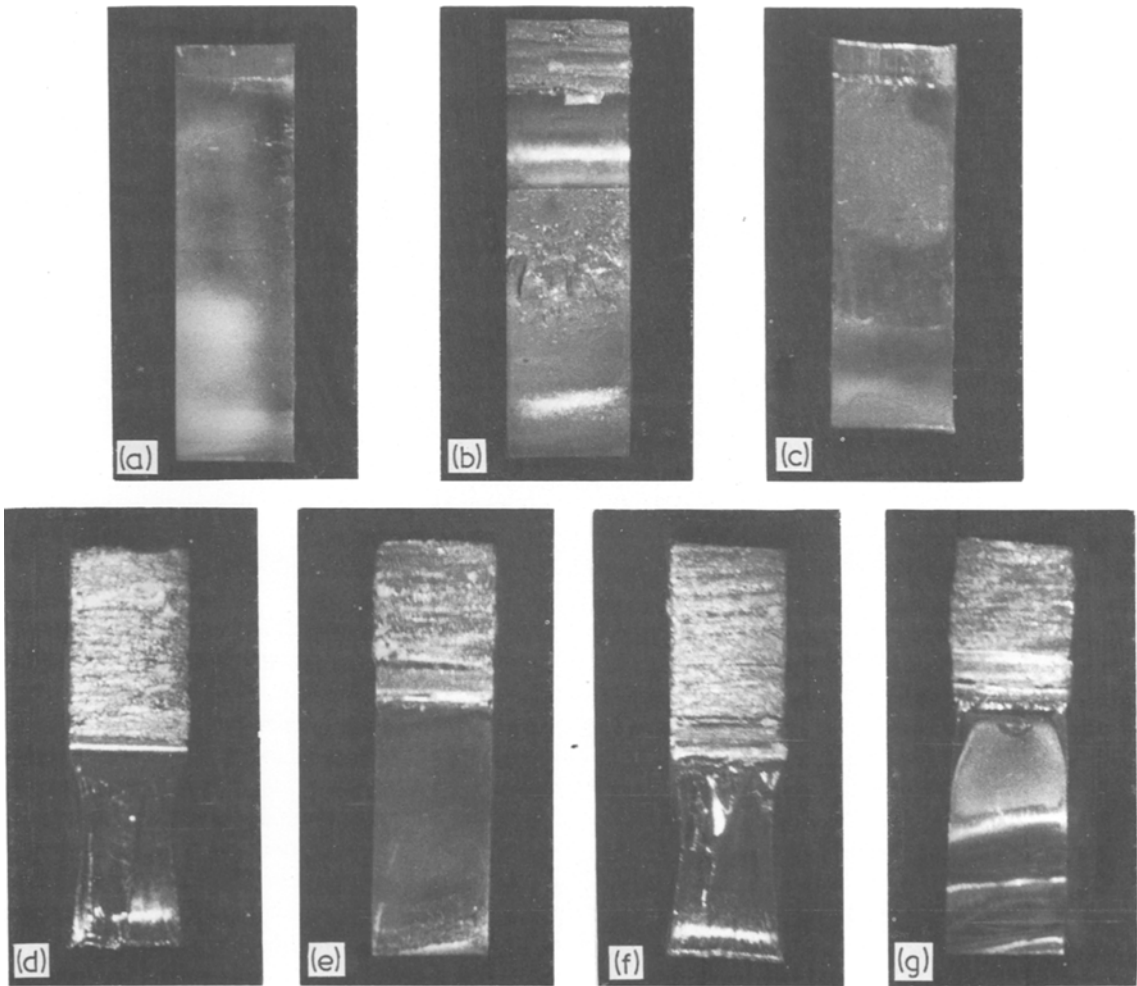


Figure 3 The fracture surface. (a) PMMA razor-notched, (b) PMMA blunt-notched, (c) PC razor-notched, (d) PC notch tip radius of 0.04 cm, (e) PC intermediate notch tip radius, category A' failure, (f) PC intermediate notch tip radius, ductile failure, (g) PC intermediate notch tip radius, brittle with ductile zone.

[10–12]. Observation of these surfaces showed that the amount of surface roughness increased as the speed of acceleration of the crack increased, i.e. as the amount of stored elastic energy for failure increased. In general, though, failure occurred on a planar front.

The razor-notched specimens of PC (Fig. 3c) show identical fracture surfaces to the razor notched specimens of PMMA. The mirror zone covers the whole specimen, and it is clear that the mode of fracture is identical.

The PC specimens with notch tip radius of ~ 0.04 cm show a much higher fracture toughness than the razor-notched specimens, and showed a very different fracture surface. Fig. 3d shows that in this case there is considerable plastic flow in the crack propagation region. We have termed this

ductile failure and denoted it as category B in Fig. 2, as distinct from brittle failure which we denote as category A.

The failure of specimens with notch tip radii in the range between 0.018 and 0.026 cm is much more complex. Three distinct types of fracture surface are observed, corresponding to the division of the fracture toughness values into three distinct groups as shown in Fig. 2. Specimens with the lowest fracture toughness, indicated by A' in Fig. 2, show the same clean fracture surfaces as the razor notched specimens of category A. A typical photograph is shown in Fig. 3e which is to be compared with the fracture surface of the blunt-notched impact specimen of PMMA shown in Fig. 3b. The comparison with PMMA is important because it was shown in the previous paper [4] that

the failure of the PMMA specimens is more correctly analysed in terms of a critical stress at the root of the notch, rather than by fracture mechanics in terms of fracture toughness.

The second group of PC specimens in this range of notch tip radii fail at comparable fracture toughnesses to those of notch tip radii 0.039 cm, which always show what we have termed ductile failure. The fracture surfaces are also identical as can be seen by comparing that of a specimen in this region shown in Fig. 3f with Fig. 3d. We have termed these specimens category B' to denote their kinship with those in category B.

Finally, there is a group of specimens which show fracture toughnesses intermediate between those of categories A' and B'. The fracture surfaces of these specimens, as illustrated in Fig. 3g, show a small yield zone at the tip of the crack which has been formed, extending a small distance along the advancing crack front, on the surfaces of the specimen. We have denoted such specimens as category C in Fig. 2.

In view of these striking observations of the different types of failure occurring in these impact tests in PC, it seems appropriate to discuss the failure of specimens in each of the five different categories separately, and this will now be done.

4.2. Detailed analysis for higher molecular weight grade PC

4.2.1. The razor-notched specimens

In the initial broad survey of the results, these were all analysed in terms of fracture toughness. The examination of fracture surfaces, and the evident analogies with PMMA, suggest that this analysis will definitely be appropriate for the razor-notched specimens. In Fig. 4 the fracture toughness K_{IC} (plane strain) for the higher mol-

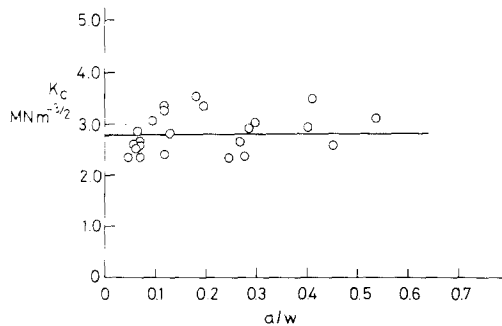


Figure 4 Impact fracture toughness of high molecular weight polycarbonate (razor-notched samples).

ecular weight grade specimens is plotted as a function of the reduced crack length (a/w) to confirm the consistency of the fracture toughness measurements over a wide variation of crack length. A plot of calculated fracture energy against experimental fracture energy (Fig. 5) gives a straight line with an intercept of 0.006 Nm, which is attributed to the kinetic energy contribution to the measured impact energy. The measured value of K_{IC} is $2.84 \text{ MN m}^{-3/2}$ which agrees well with other estimates [6].

4.2.2. The blunt-notched specimens

At the other extreme, there are the specimens which fail with large plastic flow on the fracture surface. The results in Fig. 2 show that a fracture toughness value of $19 \text{ Nm}^{-3/2}$ can be obtained which is independent of notch tip radius. The specimen fails with considerable plastic flow, reminiscent of the failure of amorphous polyethylene terephthalate (PET) in cleavage tests at room temperature [13]. The fracture toughness has been examined as a function of reduced crack length, and the composite set of results, shown in

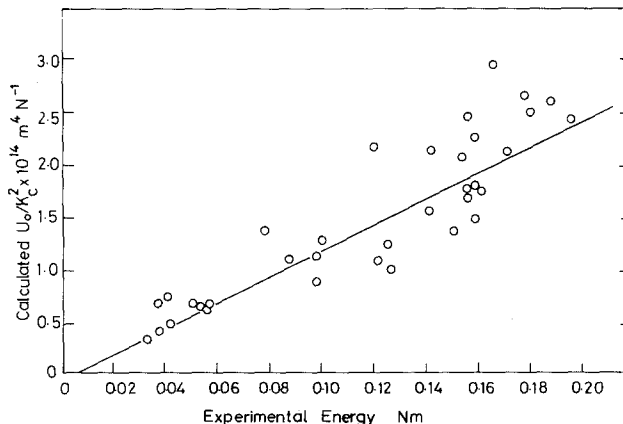


Figure 5 Calculated values of U_0/K_{IC}^2 versus experimental fracture energy for razor-notch impact tests on high molecular weight polycarbonate.

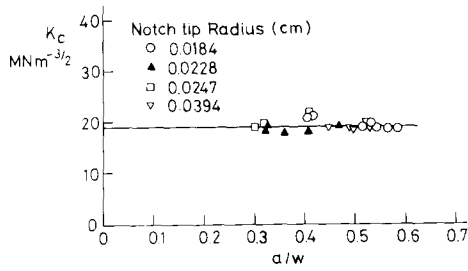


Figure 6 Impact fracture toughness tests on high molecular weight polycarbonate, ductile failure.

Fig. 6, confirm the validity of the analysis in terms of fracture toughness.

4.2.3. The blunt-notched specimens of intermediate fracture toughness

As has already been indicated, the failure of specimens with notch tip radii less than 0.03, but greater than 0.015 cm, presents a much more complex problem. Fig. 2 shows that if the results for the higher molecular weight grade are analysed in terms of fracture toughness, the fracture toughnesses fall into three distinct regimes: (a) below $5 \text{ MN m}^{-3/2}$, (b) between 5 and $10 \text{ MN m}^{-3/2}$, and (c) above $16 \text{ MN m}^{-3/2}$. We have already discussed the behaviour of those specimens which fall into the regime of highest fracture toughness in Section 4.2.2 above. These are the specimens denoted by B' in Fig. 2 and show plastic flow on the fracture surface. The behaviour of specimens with fracture toughnesses in the two other regimes will now be discussed separately, for reasons which will become apparent.

4.2.3.1. Intermediate fracture toughness: brittle fracture. The blunt-notched specimens with the lowest fracture toughness (category A' in Fig. 2) show fracture surfaces with no plastic zone and no yielding, only a flat mirror area. The measured fracture toughness is, however, significantly greater than that measured for the razor-notched specimens and, as can be seen from Fig. 2, varies with notch tip radius. The fracture toughness at constant notch tip radius appears to increase somewhat with increasing notch length, which is shown in Fig. 7. We have therefore explored the possibility that the situation for these blunt-notched specimens of PC is similar to that which was observed for blunt-notched specimens of PMMA, where it was shown that failure should not be interpreted as a critical stress intensity criterion but in terms of a critical stress at the root of the

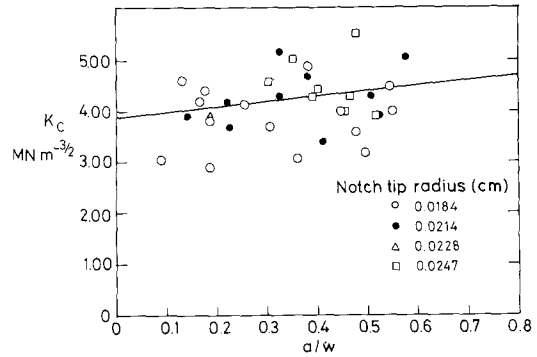


Figure 7 Fracture toughness K_{IC} versus a/w for high molecular weight polycarbonate. Brittle failure, category A', analysed as fracture toughness.

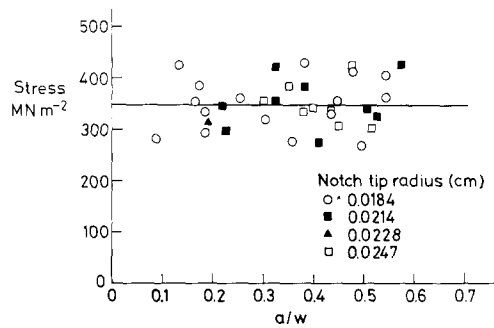


Figure 8 Charpy impact tests on high molecular weight polycarbonate, intermediate notch tip radii, brittle fracture, analysed as the stress at the root of the notch.

notch. Fig. 8 shows the calculated values of this maximum stress, derived using the method outlined in Section 3.2 above, as a function of reduced crack length for the various notch tip radii. Although the maximum stress values show considerable scatter there is now no systematic variation with either crack length or notch tip radius. It is therefore a distinct possibility that the results are consistent with a constant stress criterion. The value of this stress is, however, $\sim 350 \text{ MN m}^{-2}$, which is rather higher than would be expected in terms of the craze stress, extrapolating the direct tensile craze stress measured at low strain-rate to a value expected for the impact test. This assumes that the critical stress is the stress required to reach the craze stress at the tip of the crack. It is possible that there is a more complicated situation. This apparent stress at the crack tip could reflect a situation where, because of the ductile nature of PC there is some plastic flow at the actual crack tip relieving the stress there. The stress then only reaches the craze stress at a point some way in the material where the apparent stress at the crack tip

is significantly higher. At this juncture these ideas are speculative as no evidence of an initial yielded zone was observed in an optical microscope.

4.2.3.2. Intermediate fracture toughness: yield zone near surface. Fig. 3g shows the fracture surface of a typical specimen in category C of Fig. 2. It can be seen that in this case small yield zones have formed on the surfaces of the specimen at the tip of the crack as also reported by Mills [14]. These yield zones extend a small distance along the advancing crack front, and are no longer present in the region where the crack has accelerated. The difficulty in applying a fracture mechanics approach is highlighted by examination of the results in Fig. 2, where the calculated values of K_C vary with notch tip radius, and by Fig. 9, where the values of K_C for constant notch tip radius can be seen to vary with reduced notch length.

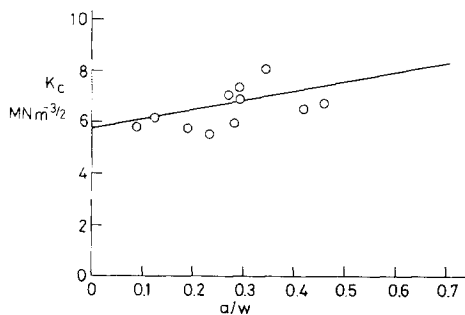


Figure 9 Impact fracture toughness of high molecular weight polycarbonate, brittle with ductile zone. Notch tip radius 0.0184 cm.

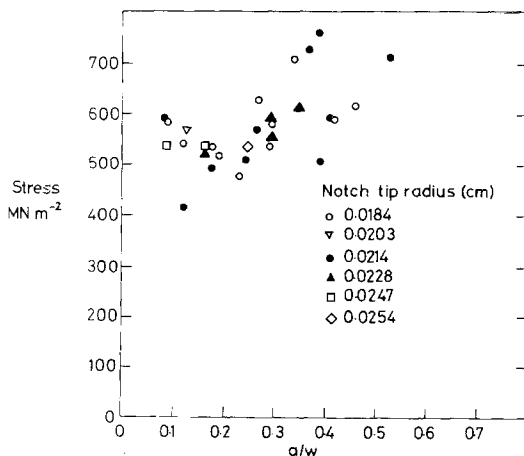


Figure 10 Charpy impact tests on high molecular weight polycarbonate. Intermediate notch tip radii, brittle with ductile zone, analysed as the stress at the root of the notch.

We therefore next consider the alternative hypothesis that failure occurs at a critical stress at the root of the notch. The results are shown in Fig. 10, and merely show a large scatter about a mean value of 560 MN m^{-2} . Although this might appear to provide some support for the idea that fracture relates to a critical stress, the value of 560 MN m^{-2} is much larger than would be expected for the yield stress even at the very high strain-rate of the impact test. Two further explanations have, therefore, been examined.

In the first instance, it was attempted to analyse the behaviour of these specimens in terms of fracture toughness, following the approach of Plati and Williams [6], who suggested that PC can show a combination of plane strain and plane stress fracture modes. From the impact measurements on the razor-notched and very blunt-notched specimens, the corresponding critical strain energy release rates for the plane strain and plane stress situations can be calculated. These were found to be 3.7 kJ m^{-2} (plane strain) and 164 kJ m^{-2} (plane stress) respectively. The areas of the two zones on the fracture surface were measured and showed that the yielded zone forms between 2 and 3% of the total surface area for short cracks and 3 and 4% for long cracks. Using these values for the plane strain and plane stress critical strain energy release rates, the average value of G_c for these specimens lies between 4.68 and 5.22 kJ m^{-2} . These values for G_c are equivalent to fracture toughness values in the range 3.2 to $3.4 \text{ MN m}^{-3/2}$, which are very considerably lower than the values of 5.9 to $9.2 \text{ MN m}^{-3/2}$ calculated directly from the impact data.

The final explanation is similar to this last approach but in this case, rather than taking the strain energy release rate over the whole area of crack propagation, the initial widths of the shear lips are considered. Fig. 11 shows the measured shear lip width at the tip of the initial crack (i.e. the maximum lip width) plotted against the measured G_c value. The straight line shown on the graph passes through two points, (a) the point represented by zero shear lip width and a strain energy release rate of 3.7 kJ m^{-2} which is a totally plane strain fracture, and (b) the point represented by 3 mm shear lip width and a strain energy release rate of 164 kJ m^{-2} , i.e. a totally plane stress fracture. As may be seen, the points fall in close proximity to this line leading to the following conclusion; the fracture toughness of these speci-

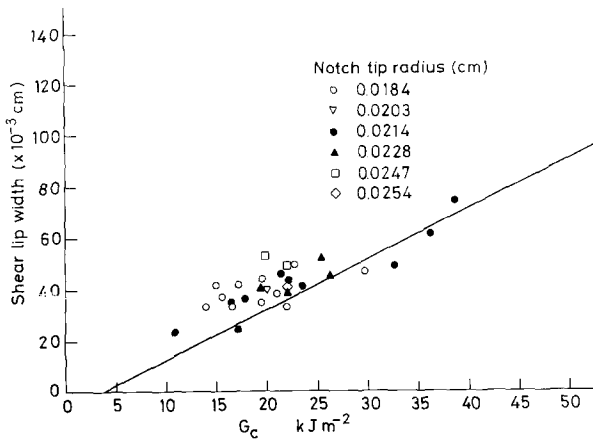


Figure 11 Shear lip width as a function of measured critical strain energy release rate, high molecular weight polycarbonate.

mens is governed by the instantaneous strain energy release rate at the instant that the movement of the crack is initiated. At this point the strain energy release rate must satisfy the combination of the two operating effects (plane stress and plane strain) and when this occurs the fracture begins to propagate. As the crack front propagates it accelerates in an unstable manner causing catastrophic failure. This mode of failure is similar to the constant maximum fracture stress approach in that an initiation criterion is proposed, further energy supply not being necessary since the specimen contains more than sufficient stored elastic energy for total failure. It is suggested that the reason for the instability is, in this case, that once the crack has started to move, the effective strain-rate of the test increases, since strains are now even more localised in the tip of the advancing crack. This causes the crack to accelerate, producing even smaller yielded zones (since at higher speeds the propensity to brittle fracture at the expense of ductile failure is increased). This leads to further acceleration of the crack and catastrophic failure.

4.5. Impact behaviour of lower molecular weight PC

Fig. 12 shows the results for the lower molecular weight grade PC, analysed as a fracture toughness test, plotting fracture toughness as a function of notch tip radius. Again there are several categories of failure and inspection of the specimens confirms that the fracture surface features are similar to those shown in Fig. 3.

As for higher molecular weight material, the razor-notched specimens (category A) can be correctly analysed in terms of fracture toughness. The fracture toughness was plotted as a function

of reduced crack length and shown to be constant with a value of $2.6 \text{ MN m}^{-3/2}$. This is significantly lower than the value obtained for the high molecular weight specimens. A separate study of the craze shape observed in slow cleavage fracture of these PC specimens [15] shows that these differences between the two grades of PC (and their difference from PMMA) relate to changes in both the craze stress and the crack opening displacement at the tip of the craze.

For very blunt notch tip radii, there are again specimens in category B which fail with large plastic flow. The fracture toughness analysis gave

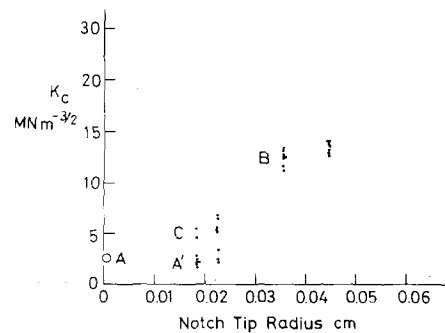


Figure 12 Impact fracture toughness of low molecular weight polycarbonate.

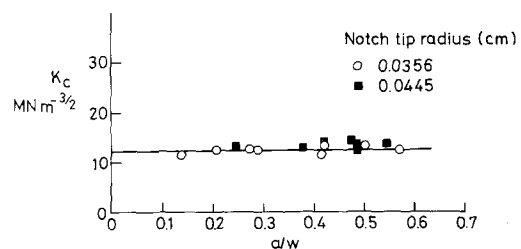


Figure 13 Impact fracture toughness tests on low molecular weight polycarbonate, ductile failure.

a value of $11.5 \text{ MN m}^{-3/2}$, which was constant both with varying notch tip radius and with reduced crack length (Fig. 13). This value for fracture toughness is considerably less than the value of $19 \text{ MN m}^{-3/2}$ obtained from the higher molecular weight polymer. The tensile yield measurements (see Table I) showed that the yield stresses of the two grades are indistinguishable. This is similar to data for PET, where it was found that the yield stress was unaffected by changes in molecular weight [16]. The marked difference between the fracture toughnesses of the two PC grades can, therefore, be attributed to differences in the extensibility to break of the two polymers. It seems likely that the failure mode is similar to rupture of a constrained element in tension, as in PET [13].

Finally, we consider the failure of specimens with intermediate notch tip radii. For low molecular weight material, failures in categories A and C only were observed. As in higher molecular weight material, category A failure was consistent with a critical stress at the root of the notch (Fig. 14). The collected results gave a mean value of 180 MN m^{-2} for this critical stress. It is instructive to consider this result in the light of the values for the critical stresses measured in impact tests for high molecular weight PC (350 MN m^{-2}) and PMMA (220 MN m^{-2}) [4], and to compare also the slow speed tensile crazing stresses of these materials shown in Table I. The low molecular weight PC and the PMMA show similar values for both the critical stress in the impact test and the crazing stress whereas the higher molecular weight material shows considerably higher values for both parameters. This strengthens the argument that the critical failure stress as measured in the impact test does indeed relate to the crazing stress of the material. In support of this, it can also

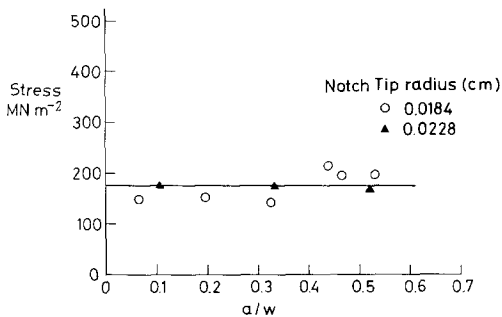


Figure 14 Charpy impact tests on low molecular weight polycarbonate, intermediate notch tip radii, brittle fracture, analysed as the stress at the root of the notch.

TABLE I Comparison of crazing and yield stresses for PC and PMMA (MN m^{-2})

	PC (Bayer Makrolon Grade 2803)	PC (Bayer Makrolon Grade 2400)	PMMA (ICI Ltd Perspex cast sheet)
Crazing stress	59.5	47	48
Yield stress	61	60	—
Critical stress in impact test	350	180	220

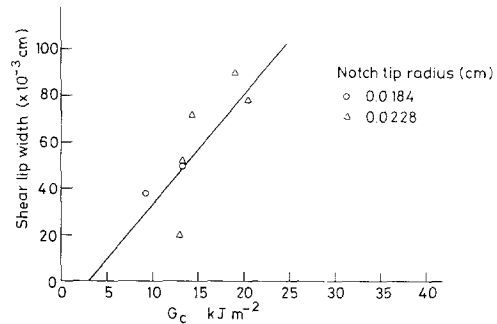


Figure 15 Shear lip width as a function of measured critical strain energy release rate, low molecular weight polycarbonate.

be added that the value of 220 MN m^{-2} obtained for PMMA compares well with a value of 200 MN m^{-2} which is obtained if the data of Bauwens-Crowet [17] for this material is extrapolated to a strain-rate of 500 sec^{-1} . (This strain rate is obtained from a linear elastic analysis of the blunt notched tests.)

For the low molecular weight material, few specimens fell into the category C failure mode. It has been possible, however, to compare the failure of these with the higher molecular weight material using the same procedure as before. Fig. 15 shows the measured shear lip width plotted against measured G_c but the paucity of data does not allow a definitive result. As before, the line joining the plane stress and plane strain G_c values is included and, although considerable scatter is shown, it is not unreasonable to conclude that these results can be explained on a similar basis to those for the higher molecular weight PC.

5. Conclusions

These impact tests on PC show that only in the case of razor-notched specimens is it possible with complete certainty to interpret the data directly in terms of fracture toughness. In our tests, the specimens with the bluntest notches also gave

constant fracture toughness values, but at a much higher level, corresponding to a different mode of failure. For intermediate notch tip radii the situation is much more complex and is certainly molecular weight-dependent. It has been shown that in this case some specimens will fail in the ductile fracture mode in an identical fashion to the very blunt-notched specimens. In the remainder, either a brittle failure mode corresponding to a critical stress can apply, or the initial strain energy release rate is the critical parameter of failure.

In this paper we have not attempted to consider the reasons for the particular distribution of different failure modes observed for specimens of intermediate notch tip radii. It is clear that this depends on the nature of the initial flaw distribution, which only razor notching is sufficiently severe to eliminate. Our results also indicate that it is likely to depend on other material parameters like the craze stress, the lower craze stress of the lower molecular weight PC leading to more brittle failures. This aspect of the work is clearly deserving of further investigation, which is now being undertaken.

References

1. H. R. BROWN and I. M. WARD, *J. Mater. Sci.* **8** (1973) 1365.
2. H. R. BROWN, *ibid* **8** (1973) 941.
3. G. P. MARSHALL, J. G. WILLIAMS and C. E. TURNER, *ibid* **8** (1973) 949.
4. R. A. W. FRASER and I. M. WARD, *ibid* **9** (1974) 1624.
5. K. GOTHAM, unpublished work presented to the Conference "Designing to Avoid Mechanical Failure", Cranfield (January, 1973).
6. E. PLATI and J. G. WILLIAMS, *Polymer* **16** (1975) 915.
7. G. A. ADAMS, A. CROSS and R. N. HAWARD, *J. Mater. Sci.* **10** (1975) 1582.
8. G. R. IRWIN and J. A. KIES, *Welding J. Res. Suppl.* **33** (1954) 1935.
9. H. NEUBER, "Theory of Notch Stresses" (Julius Springer, Berlin, 1937).
10. I. WOLOCK, J. A. KIES and S. B. NEWMAN, "Fracture Phenomena in Polymers", presented to the "Fracture" Conference, Swampscott, Mass., USA, April 1959 (MIT Press, 1959).
11. E. H. ANDREWS, "Fracture in Polymers" (Oliver & Boyd, Edinburgh, 1968).
12. S. B. NEWMAN and I. WOLOCK, *J. Appl. Phys.* **29** (1958) 49.
13. J. S. FOOT and I. M. WARD, *J. Mater. Sci.* **7** (1972) 367.
14. N. J. MILLS, *ibid* **11** (1976) 363.
15. R. A. W. FRASER and I. M. WARD, unpublished work.
16. J. M. STEARNE and I. M. WARD, *J. Mater. Sci.* **4** (1969) 1088.
17. C. BAUWENS-CROWET, *ibid* **8** (1973) 968.

Received 16 June and accepted 19 July 1976.